Induction of ciliary orientation by matrix patterning and characterization of mucociliary transport

Patrick R. Sears,[1] Ximena M. Bustamante-Marin,[1] Henry Gong,[1] Matthew R. Markovetz,[1] Richard Superfine,[2] David B. Hill,[1,3] and Lawrence E. Ostrowski[1,4,*]

[1]Marsico Lung Institute, [2]Department of Applied Physical Sciences, [3]Department of Physics and Astronomy, and [4]Department of Pediatrics, University of North Carolina, Chapel Hill, North Carolina

ABSTRACT   Impaired mucociliary clearance (MCC) is a key feature of many airway diseases, including asthma, bronchiectasis, chronic obstructive pulmonary disease, cystic fibrosis, and primary ciliary dyskinesia. To improve MCC and develop new treatments for these diseases requires a thorough understanding of how mucus concentration, mucus composition, and ciliary activity affect MCC, and how different therapeutics impact this process. Although differentiated cultures of human airway epithelial cells are useful for investigations of MCC, the extent of ciliary coordination in these cultures varies, and the mechanisms controlling ciliary orientation are not completely understood. By introducing a pattern of ridges and grooves into the underlying collagen substrate, we demonstrate for the first time, to our knowledge, that changes in the extracellular matrix can induce ciliary alignment. Remarkably, 90% of human airway epithelial cultures achieved continuous directional mucociliary transport (MCT) when grown on the patterned substrate. These cultures maintain transport for months, allowing carefully controlled investigations of MCC over a wide range of normal and pathological conditions. To characterize the system, we measured the transport of bovine submaxillary gland mucin (BSM) under several conditions. Transport of 5% BSM was significantly reduced compared with that of 2% BSM, and treatment of 5% BSM with the reducing agent tris(2-carboxyethyl)phosphine (TCEP) reduced viscosity and increased the rate of MCT by approximately twofold. Addition of a small amount of high-molecular-weight DNA increased mucus viscosity and reduced MCT by ∼75%, demonstrating that the composition of mucus, as well as the concentration, can have significant effects on MCT. Our results demonstrate that a simple patterning of the collagen substrate results in highly coordinated ciliated cultures that develop directional MCT, and can be used to investigate the mechanisms controlling the regulation of ciliary orientation. Furthermore, the results demonstrate that this method provides an improved system for studying the effects of mucus composition and therapeutic agents on MCC.

SIGNIFICANCE   Mucociliary clearance is the process whereby the coordinated activity of thousands of cilia interact with and propel mucus from the airways, removing inhaled pathogens and toxins from the pulmonary system. Our understanding of how cilia align and how they interact with the viscoelastic mucus to efficiently clear the airways is incomplete. We demonstrate that a pattern of ridges or grooves introduced into a collagen substrate can induce human airway epithelial cells to orient their cilia and transport mucus in a predetermined path. Furthermore, we examine how changes in mucus rheology and composition affect transport. These studies show that ciliary alignment can be regulated by the extracellular matrix and enables investigations of new treatments for improving mucociliary clearance in muco-obstructive lung diseases.

INTRODUCTION

Mucociliary clearance (MCC) is a critical innate defense mechanism that is essential to maintain the health of the pulmonary system (1,2). Through the integrated processes of fluid secretion and absorption, the secretion of large mucin biopolymers and other proteins that compose the viscoelastic mucus, and the proper orientation, coordination, and regulation of ciliary activity, the MCC system

continuously captures and removes pathogens and other harmful materials from the airways. The importance of MCC is clearly illustrated by diseases in which impaired MCC is central to disease pathogenesis (3). For example, in cystic fibrosis (CF), the absence or reduced function of the CF transmembrane conductance regulator protein results in dehydration of the airway surface liquid and the accumulation of a thick, viscous mucus that is difficult to clear by MCC or cough (4). The accumulated mucus becomes a nidus for infection, inflammation, and increased mucin production, setting in motion a vicious cycle of lung infection and damage. Primary ciliary dyskinesia is a rare disease caused by genetic defects that impair the function of the motile cilia that line the airways, resulting in reduced or absent MCC, leading to recurrent airway infections (5). Furthermore, impaired MCC also plays a role in the pathogenesis of other chronic diseases, including chronic obstructive pulmonary disease and asthma (3,6). A more complete understanding of the MCC system and how it fails in different disease states will allow the development of specific and efficient therapies to improve MCC and reduce morbidity and mortality.

Currently, the most direct method of studying MCC is to measure the clearance of radiolabeled particles from human subjects over time (7). In a typical study, a subject inhales nonabsorbable technetium-99m (^{99m}Tc)-labeled sulfur-colloid particles and images of the lungs are obtained with a γ-camera over a series of time points after the inhalation. The disappearance of the ^{99m}Tc signal over time is taken to represent the rate of MCC. Although this method provides a direct measure of MCC in humans, the technique requires a high level of expertise and is not widely available. Multiple different methods have been utilized to measure MCC in animal models, including measuring the disappearance of radioactive particles as described above (8,9) and tracking the transport of fluorescent or other particles, either in live animals or in ex vivo (excised) tissues (e.g., (10,11). Although these and other methods provide valuable information, they each have limitations, including the use of highly specialized equipment or techniques (e.g., synchrotron (12), optical coherence tomography (13)), the requirement to add large volumes of fluid to the airway surface, and/or the inability to perform repeat studies on the same animal.

As an alternative to animal models, many investigators have utilized well-differentiated air/liquid interface (ALI) cultures of human airway epithelial (HAE) cells to study aspects of MCC in vitro. Occasionally, these cultures have been shown to spontaneously coordinate their ciliary activity to produce areas of circular mucociliary transport (MCT), colloquially referred to as "mucus hurricanes" (14). ALI cultures have been used to investigate MCT in a wide range of studies, particularly in relation to CF (e.g., (15–18)) and toxic exposures (e.g., (19,20)). In addition, several investigators have used ALI cultures to measure

flow by tracking fluorescent particles over short distances (micrometers or millimeters (21)). We recently reported that by including an insert in the center of the culture membrane to form a circular track (i.e., an MCT device (MCTD)), we could increase the percentage of ALI cultures that developed complete circular transport (CCT) by approximately fivefold (22). In addition to increasing the percentage of cultures demonstrating transport, the MCTD (or "racetrack" cultures), allow for the directional measurement of MCT under controlled conditions, measurement of MCT over longer distances (centimeters), and repeat measurements of the same culture under different conditions over extended time periods. However, because the percentage of cultures that developed CCT was still relatively low under these conditions (∼25–45%), we explored other modifications to our protocol to attempt to increase the number of cultures developing CCT. Here, we report that by introducing a pattern of ridges and grooves into the collagen matrix used to prepare the MCTD, more than 90% of cultures studied demonstrated coordination of their cilia and CCT. We further demonstrate the utility of this system by exploring the effects of different modifications of the mucus layer, including mucin concentration, treatment with a reducing agent, and addition of genomic DNA, on the rate of transport. Importantly, we find that the inclusion of a small amount of DNA in the mucus causes a disproportionately large reduction in transport rate.

MATERIALS AND METHODS

A Supporting materials and methods section is provided in the online supplemental materials.

Culture of HAE cells

Primary HAE were obtained from the UNC Cell and Tissue Culture Core Facility under protocols approved by the UNC Institutional Review Board, and cultured as previously described (23,24). Briefly, first, passage HAE cells (250,000 cells/cm^2) were plated on 30 mm Millicell Culture Inserts (PICM03050; MilliporeSigma, Burlington, MA) coated with collagen as described below. Cells were fed both apically and basolaterally with ALI media until confluent, and then fed only from the basolateral surface. Cultures were fed three times per week for the first 2 weeks of culture and two times weekly for the remainder of the experiments.

Preparation of collagen coated inserts

MCTDs were prepared as previously described by attaching a central ring to the center of Millicell Culture Inserts using silicone sealer, creating a circular track (22). Inserts were coated with human type IV by one of two methods. In the standard procedure, a solution of collagen was added to the apical compartment of the Millicell and allowed to air dry. In the "brushed" procedure, a nylon brush was used to coat the track of the MCTD with a collagen solution. After drying, inserts were irradiated with ultraviolet light in a culture hood for 30 min and stored at 4°C until use. Additional details and videos demonstrating these procedures are described in the Supporting materials and methods section and Videos S4 and S5.

Analysis of ciliary orientation

Immunofluorescence was performed using the whole-mount staining protocol previously described (25). In brief, cultures were immunostained with rabbit anti-centriolar protein homolog B (POC1b) and mouse anti-centriolin (CNTRL). Membranes were imaged using a Nikon N-SIM microscope capturing four to six images per MCTD. Each image was taken collecting 25–35 optical sections of 0.1 μm, including the entire basal bodies-basal feet complexes of all the cells in the field of view at a resolution of 33.333 pixels/μm. Images were processed and analyzed using FIJI (26).

Rheological measurement of mucus solutions

Biophysical properties of the prepared mucus solutions were assessed at 23°C using particle tracking microrheology according to previously published methods (27). In brief, the thermally driven motion of 1-μm-diameter carboxylated Fluospheres added to prepared samples was tracked to determine their viscoelastic properties. Bead motion was recorded for 30 s at a rate of 60 frames/s using a 40× air objective on a Nikon Eclipse TE2000U microscope. Individual bead trajectories were measured automatically using a custom Python program that uses TrackPy (https://doi.org/10.5281/zenodo.34028) for bead localization and tracking. Statistical significance for particle tracking microrheology were performed using the Kurskal-Wallis test. For this analysis, each bead was considered an independent observation to observe the heterogeneity of the specimen.

Measurement of MCT rate

Cultures were visualized with a Nikon Eclipse TE2000 inverted microscope and videos were captured at 37°C with a Redlake ES-310T camera driven by SAVA software (Ammons Engineering, Clio, MI), as previously described (22). Fluorescent beads were added to the mucus solutions to more easily visualize MCT. Recorded videos were analyzed using TrackPy to determine the average speed of MCT.

RESULTS

Collagen ridges induce ciliated cell alignment

In previous studies, we found that providing HAE cells with a directional cue (i.e., a central cylinder (22)) improved the percentage of ALI cultures that developed coordinated transport. To provide an additional directional cue during differentiation of HAE cells, we used a small nylon brush to apply a thin collagen coating to preformed MCTDs. The collagen was applied in thin layers around the circular path of the MCTD and allowed to dry briefly between layers. This resulted in a series of concentric ridges/grooves in the collagen layer (Fig. 1 B) that followed the circular pattern of the MCTD. In contrast, although inserts coated with a solution of collagen showed some faint ridges/grooves, these crossed the inserts in a straight-line pattern from one edge to the other (Fig. 1 A), and we speculate that these ridges are formed by the pattern of fibers inherent in the Millicell membrane. HAEs from multiple donors were plated on MCTDs that had collagen applied either by the addition of a bulk collagen solution ("standard MCTD"), or by the brushing technique described above ("brushed MCTD"), and cultured at an ALI until well differentiated (6–8 weeks)
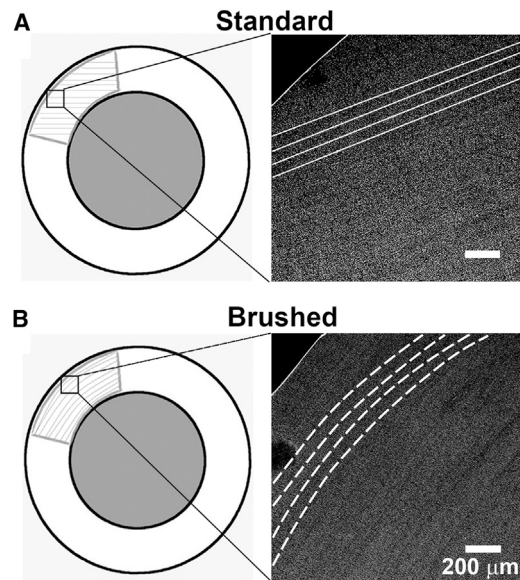

FIGURE 1 Introduction of ridges into the collagen coating. (A) Diagram (*left*) illustrating the location of a representative scanning electron micrograph (*right*) of an MCTD culture insert coated with collagen applied by bulk solution (standard). Note the straight-line pattern of ridges that extends into the side of the MCTD. (B) Diagram (*left*) illustrating the location of a representative scanning electron micrograph (*right*) of an MCTD culture insert coated with collagen by repeated application with a small brush. Note the curved lines of the ridges follow the circular track of the MCTD.

(22,28). In these studies, only a small number of the standard MCTD cultures initiated developed CCT (<10%; 13 donor samples), although many had areas of coordinated cilia that demonstrated local transport. In contrast, 85 out of 92 (~92%; 22 donor samples) consecutive cultures initiated on brushed MCTDs developed CCT (see Video S1). Once differentiated, cultures maintained CCT for months, with some cultures demonstrating transport >1 year after initiation. Between twice-weekly feedings, the apical surface of most cultures would become dry, causing transport to cease, but this was easily restored by addition of fluid and/or washing the surface to remove accumulated mucus. The transport speed of endogenous mucus varied depending on the cell donor, the amount of mucus present, and the hydration state of the culture. However, when endogenous mucus was removed by washing and replaced with a standard solution of 2% bovine submaxillary mucin (BSM), MCT was typically between 50 and 100 μm/s. This is in good agreement with previous estimates of in vivo MCT rates (29) and other studies of HAE cultures.

The proper alignment of cilia, both within and between cells, is essential for effective MCC (25,30). The direction of the ciliary beat is indicated by the alignment of the basal body-basal foot within individual cells (31). To evaluate the alignment of the basal bodies-basal feet, standard ALI cultures and brushed MCTDs that demonstrated CCT were examined by fluorescent immunocytochemistry. Basal

bodies were labeled with a POC1b antibody and basal feet were labeled with CNTRL (Fig. 2, *A* and *B*; (32)). A custom-derived script was used to detect basal body-basal foot pairs (Fig. 2, *C*, *C′*, *D*, and *D′*) and to determine the mean vector, the length of the mean vector of each individual cell (Fig. 2 *E*), and the overall length of the mean vector "r" as a measurement of the overall orientation of and degree of coordination of all the cilia in the image (Fig. 2 *F*). Multiple images from several standard and brushed MCTD cultures were analyzed. The brushed MCTD cultures displayed a significantly higher degree of ciliary coordination compared with the standard cultures, both within (0.54 ± 0.01 vs. 0.22 ± 0.01, Fig. 2 *E*) and between (0.46 ± 0.03 vs. 0.13 ± 0.013, Fig. 2 *F*) ciliated cells. In cells grown on standard inserts, some areas displayed high degrees of intracellular coordination, but the overall orientation was lower, with length of the mean vector between $0.05 < r < 0.2$ values (Fig. 2 *F*). These results confirm that the brushed collagen matrix substantially improved the intra- and intercellular coordination between ciliated cells.

Measurement of MCT

To establish a standard protocol for measuring MCT, cultures exhibiting CCT were washed to remove endogenous mucus and then a solution of 2% BSM containing fluorescent microbeads was added to the apical surface and allowed to equilibrate. The movement of the fluorescent beads was recorded at eight equally spaced fields around the culture, analyzed automatically using TrackPy software, and averaged to obtain the rate of MCT. Initial experiments compared the rate of transport of 2% BSM, representing a "healthy" mucus, to that of 5% BSM, representing the concentration of mucin that is typically observed in CF sputum (33). Cultures were washed, and the rate of transport of 2%
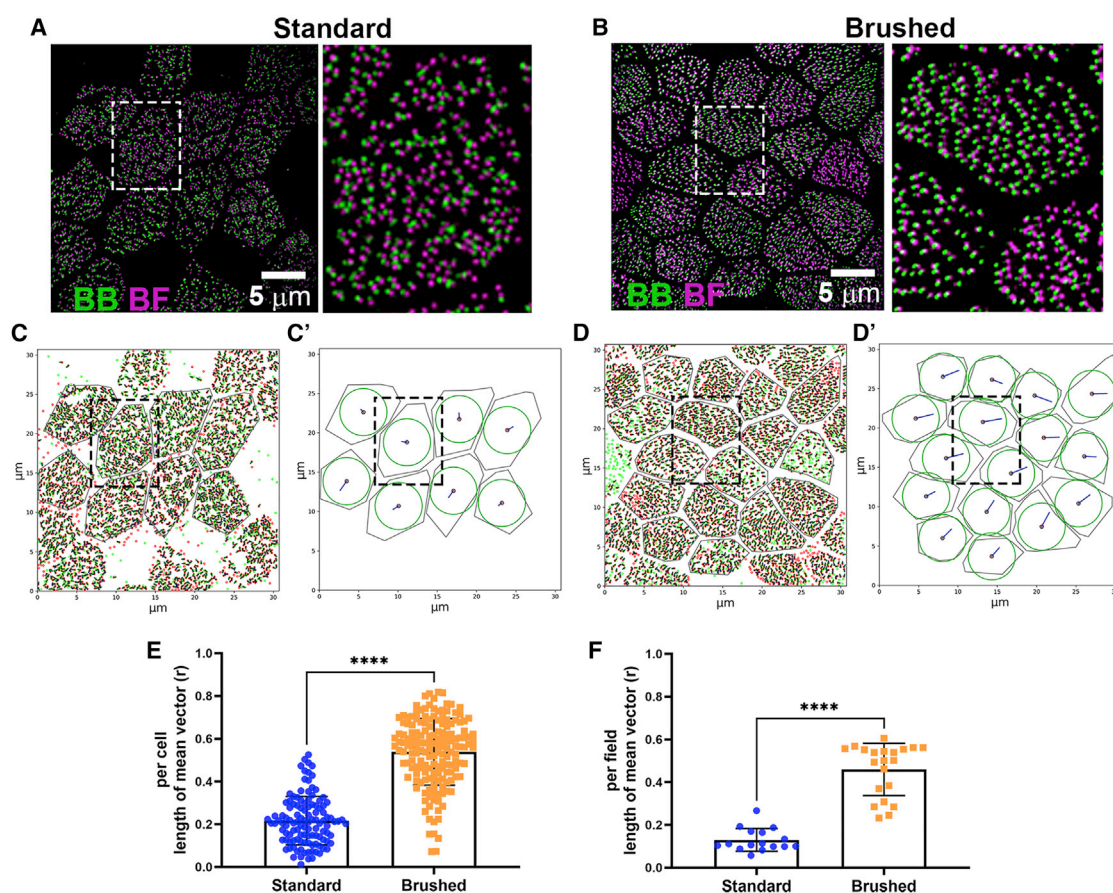

FIGURE 2 Ciliary coordination analysis. Basal bodies (BB) were labeled with an anti-POC1 centriolar protein B antibody (*green*) and basal feet (BF) were labeled with CNTRL antibody (*magenta*) to determine ciliary orientation in standard (*A*) or brushed (*B*) cultures. The boxed area in the left panel is enlarged in the right panel. (*C*, *C′*, *D*, *D′*) Representative images generated by analysis of (*A*) and (*B*) using a custom program to detect BB-BF pairs. The starting point of each vector is determined by calculating the centroid of each cell from its cell border. The green circle shows the magnitude = 1 distance for the mean vector. The unit vectors were used to quantify the degree of ciliary coordination. (*E*) Length of the mean vector (r) in individual cells from standard (n = 115 cells) or brushed (n = 165 cells) cultures. $0 < r < 1$, where 0 means no coordination and 1 means full coordination of cilia orientation. Error bars indicate SD. (*F*) Length of the mean vector (r) indicating the overall orientation of the cilia in the scanned fields from standard (n = 16 fields) or brushed (n = 21 fields) cultures. Images were collected from three cultures; each from a different donor. The quadruple asterisks indicate $p < 0.0001$ using an unpaired *t*-test with Welch correction. Error bars indicate SD.

BSM was measured. In this set of cultures, the transport rate was 74.7 ± 15.7 μm/sec, slightly faster than our earlier study in which transport of 2% BSM was 56.1 ± 5.0 μm/sec in standard cultures (22). The same culture was washed, and the rate of transport of 5% BSM was measured followed by washing and repeating the measurement of transport of 2% BSM again. As shown in Fig. 3, the rate of transport of 5% BSM was substantially reduced compared with the initial baseline transport rate of 2% BSM (see Videos S2 and S3). Importantly, the results also show that after replacing the 5% BSM solution with 2% BSM, the rate of MCT was restored to near baseline, demonstrating the reproducibility and robustness of the system.

Effect of a reducing agent on MCT

Recent reports have suggested that reducing the disulfide cross-links in mucin polymers may reduce the viscosity of airway mucus in diseases, including CF, asthma, and chronic obstructive pulmonary disease, thereby increasing MCC and improving clinical outcomes (17,34). We therefore measured the effect of the reducing agent tris(2-carboxyethyl)phosphine (TCEP) on the rheology and MCT of 2 and 5% BSM. Microrheological studies demonstrated that 10 mM TCEP significantly reduced the viscosity of both 2 and 5% BSM solutions (Fig. 4 A). Treatment with TCEP also increased the MCT rate of 5% BSM to approximately that of 2% BSM, although having no significant effect on the MCT rate of 2% BSM (Fig. 4 B). Interestingly, we find that when comparing MCT with complex viscosity (Fig. 4 C), there is a minimal viscosity that the mucus solution must surpass before MCC begins to be reduced. These
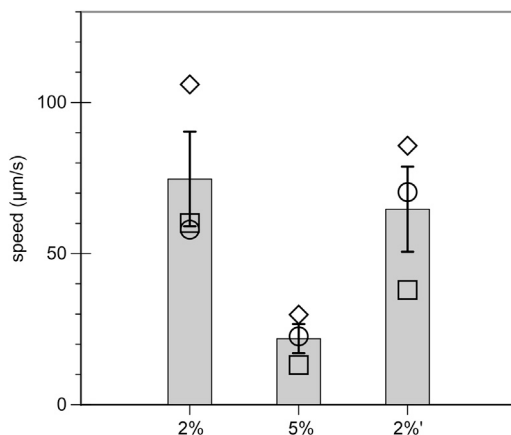

FIGURE 3 Effect of mucin concentration on MCT. The speed of MCT in 2 or 5% BSM was measured in brushed collagen MCTD cultures. MCT was measured sequentially in the same cultures (n = 3 from two different donors) using 2%, 5%, and then 2% (labeled 2%′ in the chart) BSM solutions to demonstrate the reproducibility of the system. Individual data points for three cultures are shown (*diamond*, *square*, *circle*). The columns show the mean and error bars indicate SEM. A Kruskal-Wallis one-way analysis of variance indicated the groups did not belong to the same distribution (p = 0.03) apparently because of reduced transport of the 5% BSM.

results provide further support for the development of reducing agents as mucolytic therapies for obstructive lung diseases.

Effect of DNA

In CF airways, neutrophils infiltrating in response to infection release DNA, adding another high-molecular-weight component to the mucus. The relative amount of DNA to mucin varies among CF subjects, ranging from 1:100 in children with little disease to 1:20 in adults with worse disease (35,36). Because of the higher rigidity of DNA compared with mucins, we hypothesized that small amounts of DNA could have significant effects on mucus rheology and transport. To test this, we measured the viscosity of 2, 10, and 50 mg/ml BSM solutions with and without the inclusion of small amounts of DNA. The results show that even at concentrations 20- to 100-fold less than the concentration of the mucin, the presence of DNA significantly increased mucus viscosity (Fig. 5 A). Furthermore, the rate of transport of 1% BSM was reduced ~75% by the presence of 0.04% DNA (Fig. 5 B). These results clearly show that other components of mucus, even when present at low relative amounts, can have disproportionate effects on the overall rheology and transport properties of the mucus solution.

DISCUSSION

Previous studies have shown that when cultured at an ALI, HAE cells tend to spontaneously develop areas of coordinated ciliary activity (14). However, in a typical culture insert, these areas develop in random fashion and usually do not coordinate with each other. The mechanisms controlling the coordination of ciliary beating are still poorly understood, although recent studies have highlighted the involvement of the planar cell polarity (PCP) pathway and hydrodynamic forces (37,38). Thus, Guirao et al. (37) reported that subjecting differentiating ependymal cells to an external fluid flow could orient ciliary beating in the direction of the flow. Based on our previous studies that demonstrated growing HAE cells in a circular track improved ciliary alignment, coordination, and MCT (22), we reasoned that providing the differentiating cells with an additional directional cue might further enhance their ability to coordinate. Attempts to use fluid flow to improve ciliary alignment in our experience were largely unsuccessful, likely in part because of the requirement for an ALI to obtain optimal differentiation. However, our results show that plating the cells on an MCTD with a preformed pattern introduced into the collagen substrate greatly enhanced the number of cultures that demonstrated CCT.

How the presence of ridges/groves is sensed by the dissociated airway epithelial cells and what signaling pathways are used by the cells to align their cilia are unknown. One likely possibility is that the ridges/grooves provide an axis
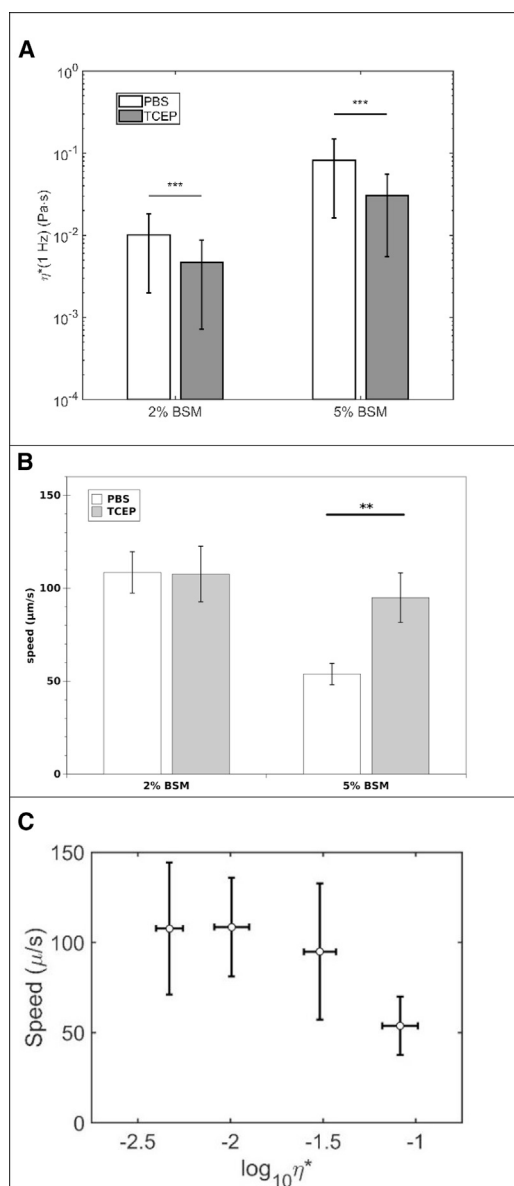
FIGURE 4 Effect of the reducing agent TCEP on rheology and MCT of BSM. (*A*) Solutions of 2% and 5% BSM were treated with or without 10 mM TCEP and rheological properties were determined (***$p <$ 0.001). Error bars indicate SD. (*B*) MCT of 2% and 5% BSM treated with or without TCEP. n = 6 cultures from three donors for 2% BSM, and n = 8 cultures from three donors for 5% BSM. **$p < 0.01$ was found by using Student *t*-test. Error bars indicate SEM (*C*) MCT versus mucus viscosity showing that there is a threshold viscosity that mucus must exceed to limit transport. Error bars indicate SD.

for the cells to align on. For example, the orientation of keratocytes has been shown to be strongly influenced by the presence of aligned collagen fibrils or nanoscale groves and ridges in the culture substrate (39,40). Binding to the collagen matrix through cellular receptors may orient the cells in the direction of the ridges, establishing a cell polarity, similar to the proximal-distal orientation of developing airway. By mechanisms that are incompletely understood,

PCP is established in the developing cells, resulting in a polarized microtubule network and asymmetric localization of PCP proteins, followed by basal body docking and ciliogenesis (38). Because flow has been shown in some cases to orient or refine ciliary beating (41), it is then reasonable to speculate that as ciliary differentiation proceeds and ciliary activity increases, the direction of ciliary beating is further refined. Although the alignment of cilia, both within and between cells, was improved in the brushed cultures, the alignment of cilia may not be as high as in vivo. For example, Vladar et al. reported a mean vector per cell of 0.83 in P5 mouse tracheas that increased with age (38). However, in these studies, orientation was determined by a different method (TEM), and we did not investigate the age of culture as a variable. Future studies to compare the development of PCP and ciliary coordination in vitro with the in vivo situation are warranted. Interestingly, in some cultures, we have observed transport moving in opposite directions on approximately one-half of the insert and forming a circular "hurricane" at their juncture. This suggests that the determination of transport direction can occur independently at different areas around the culture, and once established, may not be easily altered. This agrees with previous animal studies, in which cilia in sections of trachea that were reversed in vivo continued to beat in their original direction (42). The precise mechanisms controlling the development, refinement, and maintenance of ciliary alignment or how these processes are altered in different diseases are not known. Although the establishment of directed MCC in vivo during development occurs in a different manner than the development of CCT in an ALI culture, this system, in which the directionality of ciliary beat can be directed by a simple modification of the collagen substrate, will provide a valuable model to investigate the mechanisms involved in detail.

The method we have developed to reproducibly obtain directionally transporting cultures can also be exploited to study all aspects of MCC in a relatively simple in vitro system using HAE cells. For example, by washing off the endogenous mucus produced by the HAE cells and replacing it with a solution of known composition, we investigated the effect of mucin concentration on transport. Not surprisingly, increasing the concentration of BSM from 2 to 5% substantially reduced the transport rate, as previously reported (22). In agreement with recent studies (13,17,33), reducing disulfide bonds in the 5% mucin solution reduced the viscosity of the solution and restored transport rates to that of the 2% mucin solution. Importantly, although treating 2% BSM with the reducing agent also reduced viscosity, this did not significantly affect MCT. When comparing MCT rate with mucus viscosity, we see that MCC is decreased as the viscosity of mucus exceeds 0.01 Pa.s, or 10 times the viscosity of water, with the most pronounced result occurring as η approaches 0.1 Pa.s. We therefore speculate that the viscosity of mucus must exceed a threshold on the order of 10–100 times the viscosity of water
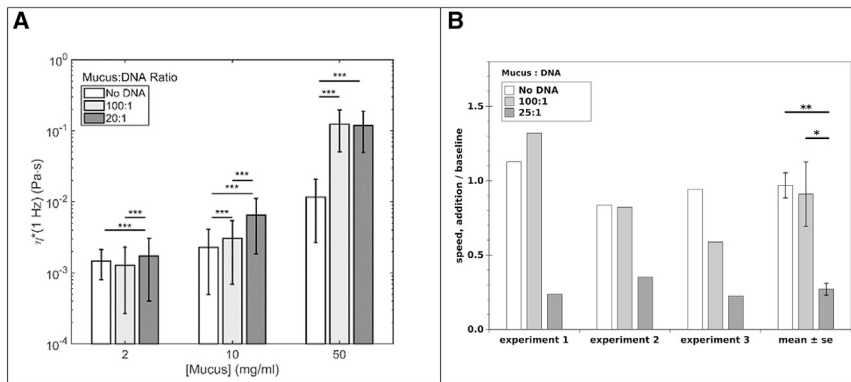
FIGURE 5 Effect of DNA on mucus rheology and transport. (*A*) Increase in rheological properties of standard solutions of BSM with increasing amounts of DNA. Error bars indicate SD. (*B*) Reduction of MCT after addition of high-molecular-weight DNA. For each test condition, the baseline rate of MCT was determined in 1% BSM followed by measuring the rate of MCT after the addition of control (PBS) or DNA solution. Figure shows three individual experiments from two donors and the average data. Error bars indicate SEM.

(i.e., 0.01–0.1 Pa. s) to slow MCC. This speculation is consistent with the previous reports of Puchelle that found CBF was slowed by viscosities greater than 0.1 Pa.s (43) and by studies of the force generation of cilia (44) that found cilia were tuned to beat against a drag force of ∼0.1 Pa. s. Therefore, we would not expect the chemical reduction of 2% BSM to affect MCC, whereas reducing 5% mucus would be predicted to have a more significant effect. Casting this result into a clinically relevant context, we would not expect the use of a mucolytic to negatively impact MCC in a healthy individual, but would expect a mucolytic to have a positive effect on patients with pathologically concentrated mucus.

To begin to examine the effect of mucus composition in disease states on MCC, we added genomic DNA to the BSM solution to simulate purulent mucus from a CF airway. Surprisingly, we found that that adding a low concentration of DNA (1% of the mucus concentration) had a significant effect on the rheology of the mucus solution, increasing viscosity significantly. This effect was further amplified by adding DNA at a concentration of 5% of the mucin concentration. Furthermore, the addition of 0.04% DNA to 1% mucin reduced MCT by ∼75%. We hypothesize that because DNA molecules are more rigid than mucin molecules, the presence of DNA has a disproportionately larger effect on mucus rheology, and subsequently, MCC. Thus, the composition of mucus, as well as its concentration, can have profound effects on the rate of transport. These results are particularly important for studies of muco-obstructive lung diseases such as CF (35) and non-CF bronchiectasis (36), both of which have elevated DNA concentrations.

The model system presented here has many advantages for studying MCC. First, the ability to induce ciliary coordination and directed mucus transport in a reproducible fashion greatly increases the number of studies that can be performed. Second, because once the cultures are entrained, they maintain transport for long periods of time (>1 year), multiple measurements can be obtained from the same culture. Third, the cultures can be easily manipulated, so

different protocols can be developed to study all aspects of MCC. For example, to measure the effect of DNA on MCT, we first measured a baseline rate of transport in cultures that were already transporting 1% BSM. The test solution (buffer, DNA) was then added to the mucus layer and allowed to mix before measuring the experimental rate of transport. Importantly, all of these can be studied under controlled, reproducible conditions in cultures of normal or diseased HAE cells. We anticipate that other improvements may further increase the utility of the system described here. For example, a previous study utilized inserts of reduced dimensions to increase throughput (19). Improvements in the composition of the media used to culture HAE cells may improve cellular differentiation to more closely resemble the in vivo airway. Moreover, additional modifications of the collagen coating, including varying the height and number of ridges and the use of a three-dimensional printer or other technology to generate the circular pattern of ridges in the collagen may further improve reproducibility.

Together, the results presented here demonstrate that this model can be adapted to study many different aspects of MCC, including the development of ciliary coordination, the effects of the composition of mucus and ciliary beat on MCC, and the regulation of ion and fluid transport. Finally, these results demonstrate that this system can be used to test and compare the effect of various therapeutics, including different combinations of agents, to improve MCC in different diseases with different mucus compositions.

SUPPORTING MATERIAL

AUTHOR CONTRIBUTIONS

L.E.O., D.B.H., P.R.S., and R.S. designed the research. P.R.S., X.M.B.-M., H.G., and M.R.M. performed research. P.R.S., X.M.B.-M., H.G., M.R.M.,

REFERENCES

1. Bustamante-Marin, X. M., and L. E. Ostrowski. 2017. Cilia and mucociliary clearance. *Cold Spring Harb. Perspect. Biol.* 9:a028241.

2. Knowles, M. R., and R. C. Boucher. 2002. Mucus clearance as a primary innate defense mechanism for mammalian airways. *J. Clin. Invest.* 109:571–577.

3. Boucher, R. C. 2019. Muco-obstructive lung diseases. *N. Engl. J. Med.* 380:1941–1953.

4. Boucher, R. C. 2007. Evidence for airway surface dehydration as the initiating event in CF airway disease. *J. Intern. Med.* 261:5–16.

5. Davis, S. D., T. W. Ferkol, …, M. W. Leigh. 2015. Clinical features of childhood primary ciliary dyskinesia by genotype and ultrastructural phenotype. *Am. J. Respir. Crit. Care Med.* 191:316–324.

6. Fahy, J. V., and B. F. Dickey. 2010. Airway mucus function and dysfunction. *N. Engl. J. Med.* 363:2233–2247.

7. Bennett, W. D., B. L. Laube, …, S. Donaldson. 2013. Multisite comparison of mucociliary and cough clearance measures using standardized methods. *J. Aerosol Med. Pulm. Drug Deliv.* 26:157–164.

8. Hua, X., K. L. Zeman, …, W. D. Bennett. 2010. Noninvasive real-time measurement of nasal mucociliary clearance in mice by pinhole gamma scintigraphy. *J Appl Physiol (1985).* 108:189–196.

9. Foster, W. M., D. M. Walters, …, L. M. Miller. 2001. Methodology for the measurement of mucociliary function in the mouse by scintigraphy. *J Appl Physiol (1985).* 90:1111–1117.

10. Rogers, T. D., L. E. Ostrowski, …, B. R. Grubb. 2018. Mucociliary clearance in mice measured by tracking trans-tracheal fluorescence of nasally aerosolized beads. *Sci. Rep.* 8:14744.

11. Francis, R., and C. Lo. 2013. Ex vivo method for high resolution imaging of cilia motility in rodent airway epithelia. *J. Vis. Exp* 50343.

12. Donnelley, M., K. S. Morgan, …, D. W. Parsons. 2014. Non-invasive airway health assessment: synchrotron imaging reveals effects of rehydrating treatments on mucociliary transit in-vivo. *Sci. Rep.* 4:3689.

13. Hancock, L. A., C. E. Hennessy, …, D. A. Schwartz. 2018. Muc5b overexpression causes mucociliary dysfunction and enhances lung fibrosis in mice. *Nat. Commun.* 9:5363.

14. Matsui, H., S. H. Randell, …, R. C. Boucher. 1998. Coordinated clearance of periciliary liquid and mucus from airway surfaces. *J. Clin. Invest.* 102:1125–1131.

15. Birket, S. E., K. K. Chu, …, S. M. Rowe. 2016. Combination therapy with cystic fibrosis transmembrane conductance regulator modulators augment the airway functional microanatomy. *Am. J. Physiol. Lung Cell. Mol. Physiol.* 310:L928–L939.

16. Button, B., M. Picher, and R. C. Boucher. 2007. Differential effects of cyclic and constant stress on ATP release and mucociliary transport by human airway epithelia. *J. Physiol.* 580:577–592.

17. Ehre, C., Z. L. Rushton, …, R. C. Boucher. 2018. An improved inhaled mucolytic to treat airway muco-obstructive diseases. *Am. J. Respir. Crit. Care Med.* 199:171–180.

18. Matsui, H., B. R. Grubb, …, R. C. Boucher. 1998. Evidence for periciliary liquid layer depletion, not abnormal ion composition, in the pathogenesis of cystic fibrosis airways disease. *Cell.* 95:1005–1015.

19. Chung, S., N. Baumlin, …, M. Salathe. 2019. Electronic cigarette vapor with nicotine causes airway mucociliary dysfunction preferentially via TRPA1 receptors. *Am. J. Respir. Crit. Care Med.* 200:1134–1145.

20. Schmid, A., N. Baumlin, …, M. Salathe. 2015. Roflumilast partially reverses smoke-induced mucociliary dysfunction. *Respir. Res.* 16:135.

21. Seagrave, J., H. H. Albrecht, …, G. Solomon. 2012. Effects of guaifenesin, N-acetylcysteine, and ambroxol on MUC5AC and mucociliary transport in primary differentiated human tracheal-bronchial cells. *Respir. Res.* 13:98.

22. Sears, P. R., W. N. Yin, and L. E. Ostrowski. 2015. Continuous mucociliary transport by primary human airway epithelial cells in vitro. *Am. J. Physiol. Lung Cell. Mol. Physiol.* 309:L99–L108.

23. Fulcher, M. L., S. Gabriel, …, S. H. Randell. 2005. Well-differentiated human airway epithelial cell cultures. *Methods Mol. Med.* 107:183–206.

24. Fulcher, M. L., and S. H. Randell. 2013. Human nasal and tracheobronchial respiratory epithelial cell culture. *Methods Mol. Biol.* 945:109–121.

25. Bustamante-Marin, X. M., W. N. Yin, …, L. E. Ostrowski. 2019. Lack of GAS2L2 causes PCD by impairing cilia orientation and mucociliary clearance. *Am. J. Hum. Genet.* 104:229–245.

26. Schindelin, J., I. Arganda-Carreras, …, A. Cardona. 2012. Fiji: an open-source platform for biological-image analysis. *Nat. Methods.* 9:676–682.

27. Markovetz, M. R., D. B. Subramani, …, D. B. Hill. 2019. Endotracheal tube mucus as a source of airway mucus for rheological study. *Am. J. Physiol. Lung Cell. Mol. Physiol.* 317:L498–L509.

28. Oltean, A., A. J. Schaffer, …, S. L. Brody. 2018. Quantifying ciliary dynamics during assembly reveals stepwise waveform maturation in airway cells. *Am. J. Respir. Cell Mol. Biol.* 59:511–522.

29. Wanner, A., M. Salathé, and T. G. O'Riordan. 1996. Mucociliary clearance in the airways. *Am. J. Respir. Crit. Care Med.* 154:1868–1902.

30. Kunimoto, K., Y. Yamazaki, …, S. Tsukita. 2012. Coordinated ciliary beating requires Odf2-mediated polarization of basal bodies via basal feet. *Cell.* 148:189–200.

31. Vertii, A., H. F. Hung, …, S. Doxsey. 2016. Human basal body basics. *Cilia.* 5:13.

32. Liu, Z., Q. P. H. Nguyen, …, V. Mennella. 2020. A quantitative superresolution imaging toolbox for diagnosis of motile ciliopathies. *Sci. Transl. Med.* 12:eaay0071.

33. Hill, D. B., R. F. Long, …, B. Button. 2018. Pathological mucus and impaired mucus clearance in cystic fibrosis patients result from increased concentration, not altered pH. *Eur. Respir. J.* 52:1801297.

34. Yuan, S., M. Hollinger, …, J. V. Fahy. 2015. Oxidation increases mucin polymer cross-links to stiffen airway mucus gels. *Sci. Transl. Med.* 7:276ra27.

35. Esther, C. R., Jr., M. S. Muhlebach, …, R. C. Boucher. 2019. Mucus accumulation in the lungs precedes structural changes and infection in children with cystic fibrosis. *Sci. Transl. Med.* 11:eaav3488.

36. Ramsey, K. A., A. C. H. Chen, …, M. A. McGuckin. 2020. Airway mucus hyperconcentration in non-cystic fibrosis bronchiectasis. *Am. J. Respir. Crit. Care Med.* 201:661–670.

37. Guirao, B., A. Meunier, …, N. Spassky. 2010. Coupling between hydrodynamic forces and planar cell polarity orients mammalian motile cilia. *Nat. Cell Biol.* 12:341–350.

38. Vladar, E. K., R. D. Bayly, …, J. D. Axelrod. 2012. Microtubules enable the planar cell polarity of airway cilia. *Curr. Biol.* 22:2203–2212.

39. Lam, K. H., P. B. Kivanany, …, D. W. Schmidtke. 2019. A high-throughput microfluidic method for fabricating aligned collagen fibrils to study Keratocyte behavior. *Biomed. Microdevices.* 21:99.

40. Teixeira, A. I., P. F. Nealey, and C. J. Murphy. 2004. Responses of human keratocytes to micro- and nanostructured substrates. *J. Biomed. Mater. Res. A.* 71:369–376.

41. Mitchell, B., R. Jacobs, …, C. Kintner. 2007. A positive feedback mechanism governs the polarity and motion of motile cilia. *Nature.* 447:97–101.

42. Tsuji, T., R. Nakamura, …, K. Omori. 2018. Long-term preservation of planar cell polarity in reversed tracheal epithelium. *Respir. Res.* 19:22.

43. Puchelle, E., J. M. Zahm, and F. Aug. 1981. Viscoelasticity, protein content and ciliary transport rate of sputum in patients with recurrent and chronic bronchitis. *Biorheology.* 18:659–666.

44. Hill, D. B., V. Swaminathan, …, R. Superfine. 2010. Force generation and dynamics of individual cilia under external loading. *Biophys. J.* 98:57–66.

Supplemental information

Induction of ciliary orientation by matrix patterning and characterization of mucociliary transport

Patrick R. Sears, Ximena M. Bustamante-Marin, Henry Gong, Matthew R. Markovetz, Richard Superfine, David B. Hill, and Lawrence E. Ostrowski

Extended Materials and Methods

Culture of human airway epithelial cells
Primary human airway epithelial cells (HAE) were obtained from the UNC Cell and Tissue Culture Core Facility under protocols approved by the UNC Institutional Review Board, and cultured as previously described[1, 2]. Briefly, first passage HAE cells (250,000 cells/cm^2 were plated on 30 mm Millicell Culture Inserts (Millipore, PICM03050) coated with collagen as described below. Cells were fed both apically and basolaterally with ALI media until confluent, and then fed only from the basolateral surface. Cultures were fed 3x/week for the first 2 weeks of culture and 2x weekly for the remainder of the experiments.

Preparation of collagen coated inserts
Mucociliary Transport Devices (MCTDs) were prepared as previously described by attaching a central ring to the center of Millicell culture inserts using silicone sealer, creating a circular track around the outside edge of the Millicell [3]. The procedure is demonstrated in Video S4. Inserts were coated with human placental type IV collagen (Sigma-Aldrich, C7521) by one of two methods. In the standard procedure, 483 uls of 750 ug/ml of collagen was added to the apical compartment of the Millicell and allowed to air dry. In the "brushed" procedure, a #2 nylon brush was used to coat the track of the MCTD in a circular direction, using a 3 mg/ml collagen solution. An approximately equal amount of collagen was applied in several applications (121 ul of 3 mg/ml stock), with time allowed between applications for air drying. After drying, inserts were irradiated with UV light in a culture hood for 30 min. and stored at 4° C until use. The procedure is demonstrated in Video S5.

Monitoring of mucociliary transport
After cultures become ciliated, they were monitored weekly for transport as follows. The cultures were washed with PBS to remove excess mucus and the wash solution is removed by aspiration, leaving enough fluid to form a ring along track edges. The culture was then placed in the incubator for at least ten minutes and checked for transport within one hour of the wash. Successful coordination is indicated by the transport of endogenous mucus (debris particles) which can be followed continuously around the MCTD in one direction. Cultures generally establish directional transport after ~4-8 weeks of culture, at which time they were used for experiments.

Measurement of mucociliary transport rate
Cultures were visualized with a Nikon Eclipse TE2000 inverted microscope equipped with a 20x ELWD objective and videos were captured at 37°C with a Redlake ES-310T camera driven by SAVA software (Ammons Engineering, Clio, MI), as previously described [3]. Fluorescent beads [Molecular Probes FluoSpheres, carboxylate modified polystyrene microspheres 1-um yellow-green (505/515), F-8823] were added to the mucus solutions to more easily visualize MCT. Mucus solutions were prepared by dissolving bovine submaxillary mucin (BSM; M3895, Sigma-Aldrich) in PBS at appropriate concentrations. Recorded videos were analyzed using TrackPy to determine the average speed of MCT.

Analysis of ciliary orientation
Immunofluorescence was performed using the whole-mount staining protocol previously described [4]. In brief, standard (n=3) and brushed (n=3) MCTD cultures were washed with

PBS 3 times to remove mucus accumulation and fixed with cold 100% methanol for 20 min on ice. After permeabilizing and blocking, the Millicell membrane was excised from the MCTD and cut into 4 pieces. Individual fragments were added to a well of a 48-well plate and incubated with 200 ul of primary antibodies rabbit-anti- centriolar protein homolog B (POC1b; 1:250 dilution, HPA038841, Sigma-Aldrich) and mouse-anti-Centriolin (CNTRL; 1:250 dilution, C-9 sc-365521, Santa Cruz Biotechnology, Inc.) mixed in blocking solution. After overnight incubation, the membranes were washed 3 times and antibody binding was detected using donkey-anti-rabbit Rhodamine Red-X (Jackson ImmunoResearch Laboratories, West Grove, PA) and donkey-anti-mouse Alexa Fluor-488 (Life Technologies). Following 2 hours of incubation, the membranes were washed and mounted on slides using ProLong Diamond antifade mounting media (Thermo Fisher).

Imaging of cultures
The cell culture membranes were imaged using a Nikon N-SIM microscope capturing 4 to 6 images per MCTD. Each image was taken collecting 25 - 35 optical sections of 0.1 μm including the entire basal bodies-basal feet complexes of all the cells in the field of view at a resolution of 33.333 pixels/μm (px/μm). Images were processed and analyzed using FIJI [5]. No detectable staining was observed for isotype matched control antibodies.

Analysis of cilia orientation
To define the x-y localization of individual basal body (channel 2, red) and basal foot (channel 1, green), the maximum intensity Z projection images were analyzed with ComDetV.04.1 plugin of Fiji. The size of the particles in both channels was set as 5px, and channel intensity at 20. Large particles were not segmented and were excluded. The maximum distance between colocalizing particles was set at 2 px. The x and y localization (in px) of the particles in channels 1 and 2 was saved in a file. The cell boundaries were traced manually using Fiji's multi-point tool making sure that the polygons defining a cell should not be closed. The boundaries (coordinates in x and y planes, in μm) were also saved in a file. To measure the ciliary orientation of individual cells and the overall orientation of all the cilia in the image we used the program Basal Body Opro written in Python and available at GitHub (https://github.com/patrick-sears/basal_body_opro). This script can be run in Windows using the QT console in the Anaconda Navigator. The script counts the number of cells, the total number of basal bodies and basal feet, and the total number of basal bodies that have a matching foot. The scripts provide unit vectors for matching (basal body) → (basal foot), and calculates the mean of all vectors and the length of the mean vector "r". The length of the mean vector represents the degree of ciliary coordination with values that fluctuate between $0 < r < 1$, were 0 means no coordination and 1 means full coordination of cilia orientation.

Rheological measurement of mucus solutions
Biophysical properties of the prepared mucus solutions were assessed using particle tracking microrheology according to previously published methods [6]. In brief, the thermally driven motion of 1 μm diameter carboxylated Fluospheres (ThermoFisher, Fremont, CA) added to prepared samples was tracked to determine their viscoelastic properties. Bead motion was recorded at 23°C for 30 s at a rate of 60 frames/s using a 40x air objective on a Nikon Eclipse TE2000U microscope. Individual bead trajectories were measured automatically using a custom Python program that uses TrackPy (doi: 10.5281/zenodo.34028) for bead localization and tracking.

Experimental protocols

– **Mucin concentration studies**

Each culture was first given a five minute wash with PBS to remove accumulated mucus. Immediately prior to starting the experiment, the culture was given another wash and 50 ul of 2% BSM as added. The culture was tilted with a rolling motion to ensure the track was completely covered with BSM and placed on the microscope stage and allowed to equilibrate for ten minutes. Videos were recorded (30 fps) from eight evenly spaced fields of view in the center of the track. The culture was washed three times to remove the BSM and allowed to recover for a minimum of thirty minutes. This procedure was then repeated first using 5% BSM and then 2% BSM.

– **Effect of mucolytic**

Each culture was first given a five minute wash with PBS to remove accumulated mucus. Immediately prior to starting the experiment, the culture was given another wash and 50 ul of test solution (BSM with or without TCEP) was added. The culture was placed on the microscope stage and allowed to equilibrate for ten minutes. Videos were recorded (30 or 120 fps) from eight evenly spaced fields of view in the center of the track. The culture was washed three times to remove the test solution and 50 ul of another test solution was added. The culture was then placed back on the stage, and allowed to equilibrate for ten minutes. Videos were then taken as before. The order of addition of test solutions was alternated, so that cultures did not receive the test solutions in the identical order.

– **Effect of DNA on mucociliary transport.**

Cultures were washed as above. Due to the length of the experiment, amiloride (100 uM) was added to the basal media to prevent dehydration of the culture surface. Fifty ul of 1% BSM was added, the culture was rolled, placed on the stage (t = 0'), and the position recorded. At t = 10', a baseline video set (see below) was taken at 120 fps. As soon as videos were done (about t = 12'), 5 ul of test solution was added. Additions were made at the opposite ends of the culture, 2.5 ul each. At t = 35', an additional video set was taken.

Video sets:

For each culture, one baseline video set was taken at t = 10' A second additional video set was taken at t = 35'. Each video set was composed of nine videos, one bright field (BF) videos for CBF and eight epifluorescence (FL) videos for transport measurements. All videos were taken in the center of the track. The BF video was taken first at the original position. Then the eight FL videos were taken at equidistant locations around the track.

Experimental sets:

Experiments were done in sets of three. In a set of three experiments, three cultures were tested. Each culture was tested on three different days with at least one day between tests. Each day, a culture had CBF and transport recorded under baseline and a single test (addition) condition. Additions were: PBS++ (control), DNA low concentration (0.10 mg/ml), DNA high concentration (0.40 mg/ml). DNA was from salmon testes (Sigma D1626). The three cultures were exposed to these additions in a different order. For example, one culture was exposed to PBS++ on the first day while another was exposed to DNA at a low concentration on the first day.

Video S4. Assembling the MCTD.

Apply glue to the central cylinder. Wipe away glue from the outer edge of the cylinder. Place it on the jig. Place the insert over the cylinder and press the insert membrane onto the cylinder. Remove the MCTD from the jig and use an applicator to spread the glue over the membrane inside the central cylinder. Set aside to dry.

Video S5. Preparing the collagen coating.

Put the volume of collagen to apply in a separate tube. Use 50 ul of collagen solution per centimeter squared of membrane. For 30 mm Millicells (23 mm membrane outer diameter) and a central cylinder with an outside diameter of 15 mm, we use 122 ul per MCTD). Dip the brush into the collagen solution. Brush the collagen onto the MCTD membrane in a circular motion. Set the MCTD aside to dry. Repeat the dip and brush for each MCTD. When all MCTDs have dried, brush again, always keeping to the same brushing direction, counterclockwise in the example shown. Continue until all the collagen has been applied. After drying, inserts are irradiated with UV light in a culture hood for 30 min. and stored at 4° C until use.

References

1. Fulcher, M.L., et al., *Well-differentiated human airway epithelial cell cultures.* Methods Mol Med, 2005. **107**: p. 183-206.
2. Fulcher, M.L. and S.H. Randell, *Human nasal and tracheo-bronchial respiratory epithelial cell culture.* Methods in molecular biology, 2013. **945**: p. 109-21.
3. Sears, P.R., W.N. Yin, and L.E. Ostrowski, *Continuous mucociliary transport by primary human airway epithelial cells in vitro.* American journal of physiology. Lung cellular and molecular physiology, 2015. **309**(2): p. L99-L108.
4. Bustamante-Marin, X.M., et al., *Lack of GAS2L2 Causes PCD by Impairing Cilia Orientation and Mucociliary Clearance.* American Journal of Human Genetics, 2019. **104**(2): p. 229-245.
5. Schindelin, J., et al., *Fiji: an open-source platform for biological-image analysis.* Nature methods, 2012. **9**(7): p. 676-82.
6. Markovetz, M.R., et al., *Endotracheal tube mucus as a source of airway mucus for rheological study.* Am J Physiol Lung Cell Mol Physiol, 2019. **317**(4): p. L498-L509.